Advances in Science and Technology Research Journal

Advances in Science and Technology Research Journal 2023, 17(2), 353–361
https://doi.org/10.12913/22998624/161884
ISSN 2299–8624, License CC-BY 4.0

Received: 2023.01.16
Accepted: 2023.03.15
Published: 2023.04.01

Influence of Water-Jet on Micro-Formed Parts Process via Nano-Indentation and SEM Analysis

James Kwasi Quaisie[1*], Philip Yamba[2], Vitus Mwinteribo Tabie[3], Anthony Akayeti[2], Jamal-Deen Kukurah[2], Abdul-Hamid Mohammed[1]

[1] Faculty of Engineering, Welding & Fabrication Department, Tamale Technical University, Tamale, 00233, Ghana

[2] Faculty of Engineering, Mechanical Engineering Department, Tamale Technical University, Tamale, 00233, Ghana

[3] Faculty of Engineering, Mechanical Engineering Department, Hila Liman Technical University, Wa, 00233, Ghana

* Corresponding author's email: jkquaisie@tatu.edu.gh

ABSTRACT

Based on the experimental study of cavitation water jet impact on micro-forming, a single round hole micro-die was used in this paper. The effect of different process parameters on the performance of AISI 304 stainless steel foil was examined, which involves the nanometer hardness, and elastic modulus. The nano-indentation tester was used to test the nano-hardness of the formed part, and the performance of the workpiece before and after the impact was analyzed. The nano-hardness and elastic modulus increased significantly with an increase in the incident pressure. When the incident pressure was 20 MPa and the impact time of 5 min, the hardness increased by at least 122%, and the elastic modulus increased by at least 76%. After the cavitation water jet shocked the metallic foil of the SEM analysis and the results indicated that, as the incident pressure increases, the surface morphology of the formed part changes from approximately spherical to spherical, and the spherical roundness increases. In addition, there were different degrees of defects at the bottom of the formed part, and as the incident pressure increased, the bottom defects became more and more obvious, from micro-cracks to micro-layer cracks.

Keywords: impact; AISI 304 stainless steel; incident pressure; metallic foil; water jet

INTRODUCTION

The high-pressure water will be forced through the cavitation nozzle by the cavitation water jet. The cavitation nucleus gathers, forms, and grows in the nozzle and jet shear layer's inner and outer low-pressure zones. Cavitation group bubbles begin to form and grow as a high-speed jet moves in their direction, eventually becoming a cavitation water jet [1]. Group bubbles in the jet collide with the target's surface, creating a high-impact pressure and stress concentration that can ultimately be exploited in the machining industry [2, 3]. Experimental and numerical research has looked into the possible issues of high-speed water jet impact. The pressure distributions of various high-speed water jet shapes impinging on the plate surface and the pressure peak computation method are derived under various assumptions [4]. Tong et al. [5] used experimental and boundary element approaches to investigate the collapse of a bubble close to a structure, particularly the intense splashing load following a jet load [6]. A study on the micro-forming process utilizing cavitation water-jet shock and various incidence pressures was carried out by Quaisie et al. [7]. The researchers' findings showed that using dynamic micro-forming techniques, the metallic foil surface morphology had good geometric topographies and no fractures or cracks.

As a result, this research proposes a shock micro-forming technology based on cavitating water jets. As compared to other forming processes, cavitating water jet shock micro-forming has the advantages of low cost, good processing stability, and significantly improved formability [8]. Cavitation clouds are created by injecting a high-velocity water jet through a nozzle into a water-filled chamber during the process. Using the cavitation bubbles produced in the jets as the driving force, the cavitation bubbles periodically flow out of the nozzle and scatter over the surface of the material to be processed, generating high-pressure shock (cavitation bubbles collapse impact loads) generated by the collapse of the bubbles [9]. High-pressure shock waves spread through the interior of the metal foil as they work on the material's surface. The yield and high-speed plastic deformation of the metal foil will occur if the peak pressure is greater than the dynamic yield strength of the metal foil. The metal foil continues to deform plastically until the peak stress reaches the dynamic yield strength. Hydraulic parameters such as upstream and downstream pressures will influence the strength of the shock and the area where it occurs in cavitating water jets [10]. Furthermore, the metal foil may be precisely copied to the form of the mold when used in conjunction with different mold shapes to achieve metal foil profiling. Also, since the collapse pressure's peak value approaches the gigapascal (GPa) amplitude range, it's ideal for the plastic formation of difficult-to-machine materials [11–13]. Furthermore, the concept of surface interfaces could be used in engineering and particularly in manufacturing systems to observe processes [14]. The tool-to-metal foil surface layer is solid-solid in the vast majority of micro metal forming processes. A liquid-solid interface is formed between the material and the tool in the cavitating water jets shock micro-forming phase. This fact brings many advantages such as low friction between the tool and the metal foil and no need for lubrication during the forming process. Additionally, the loads at the tool to metal foil interface surface are more distributed when compared to the micro-metal forming with a rigid tool. These gaps can be achieved using the cavitating water jet shocking deformation.

The purpose of the study is to utilize cavitation water jet shock to investigate Nano-indentation and SEM analysis of the AISI 304 stainless steel foil micro-forming process.

MATERIAL AND EXPERIMENTAL DETAIL

Materials

AISI 304 stainless steel foils with a thickness of 100 μm were selected for this experiment due to their widely used in microelectronic parts due to their resistance to corrosion and excellent mechanical properties. At first, the AISI 304 stainless steel foils were cut into 50 mm × 50 mm. Then, the thin metal foil was placed on the top of the die and covered the die openings completely. The AISI 304 stainless steel foil squares were cleaned of dirt with anhydrous alcohol. Then, the residual liquid was wiped off the surface of the AISI 304 stainless steel foil squares.

Forming device

Figure 1 shows the forming device which consists of a locking block, mask, seal ring, metal

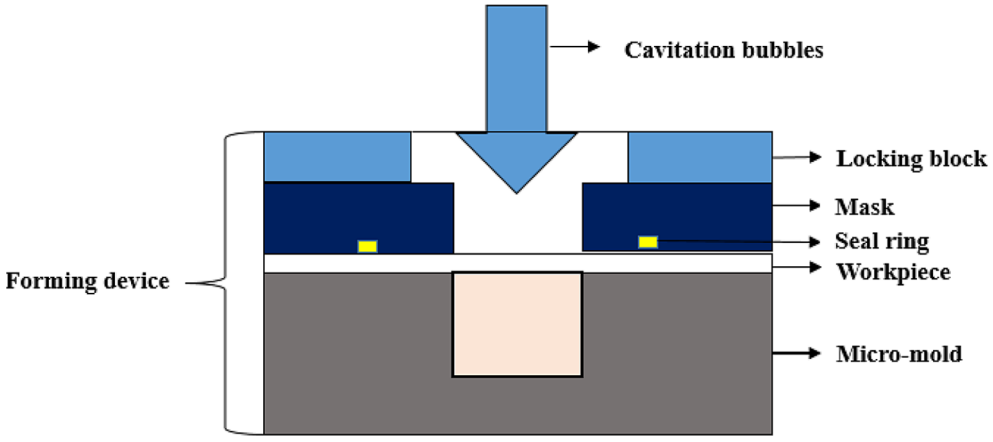

Figure 1. Schematic illustration of the forming device

foils, and micro-die. At the initial stage, the foil was placed on the top of the die, covering the die-openings completely. The metallic foil flatness should be guaranteed during the process. Next, the mask was placed on the foil and the micro-die have the same axial hole at the centre. Finally, the initial interface between the foil and the micro-die is very important, therefore the two surfaces should be firmly locked by a locking block to prevent material wrinkling. In addition, a seal ring was also applied between the foil and the mask to ensure effective sealing.

The stress diagram on the surface of the formed part is shown in Figure 2.

Experimental setup

Figure 3(a) is a schematic diagram of the experimental setup of water jet cavitation shock micro-micro-forming equipment used for the process. Tap water is stored for at least 24 hours before the experimental test in a large tank of 2.5 m × 2 m × 1.5 m size with a room temperature of 25 ± 2 ° C. A transparent water tank with a square horizontal cross-sectional area of 500 × 500 × 900 mm was used to carry out the experiments. For transparent flow purposes, the tank is made of acrylic resin. The nozzle used in this experiment was designed regarding the angular nozzle for producing the periodic behaviour of the jets of cavitation as shown in Figure 3b [15]. The nozzle was fixed in water at room temperature. The water pumped was discharged at an incident pressure of 8 to 20 MPa. The throat nozzle diameter was 1.5 mm, and the throat length L of 12 mm with an expansion angle θ of 30°. The optimum size ratio of the nozzle was d: L = 1:8 [16]. The distance between the sample workpiece was 120 mm. Inside the test cell, the specimen is placed perpendicularly to the cavitating jets. The axial distance S_L between the micro-mold cavity and the jet axis was fixed at 10 mm (the eccentricity S_L was 10 mm). A duration time of 5 minutes was selected for the performance of this experiment and with an incident pressure of 8 MPa, 12 MPa, 16 MPa and 20 MPa.

Testing methods and equipment of nano-indentation

Hardness is a comprehensive manifestation of the mechanical properties of metal materials. It represents its ability to resist the intrusion of hard objects locally. Sharifikolouei et al. [17] explored how hardness could be improved in Ti-stabilized austenitic stainless steel, and their findings on a nano-indentation study of those fibres revealed an even larger improvement in hardness, reaching an average value of 14.2 1.0 GPa. The surface hardness of micro-formed specimens measures the service life of the workpiece, wear resistance, corrosion resistance and resistance to elastoplastic deformation. It plays an important reference role and is an important parameter for the performance of materials. The cavitation water jet shock metal foil micro-forming technology is a new process that combines forming and strengthening. The high-pressure impact caused by the collapse of the cavitation bubble generates a dynamic response inside the material, which leads to plastic forming and also improves its surface hardness, the greater the amount of deformation of the material, the higher its local hardness [18]. In this section, the nano-indentation experiment was mainly used to reveal the nano-hardness distribution of the micro-formed parts. The hardness of the cross-section of the shock zone of the sample was selected to study the effect of different incident pressures on it. The nano-indentation test on the material is a test on the nanometer scale,

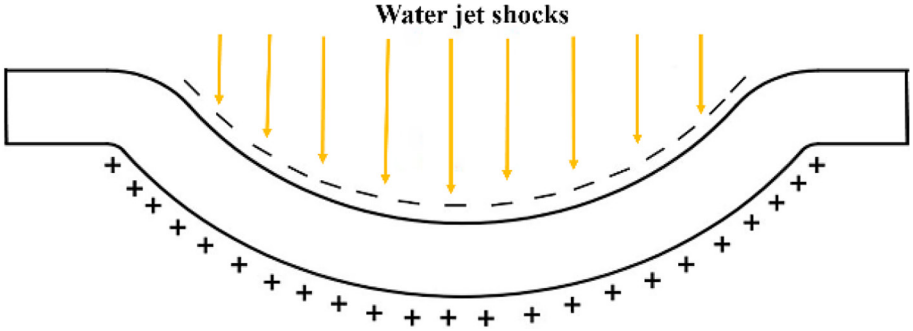

Figure 2. The surface stress distribution after cavitation shock

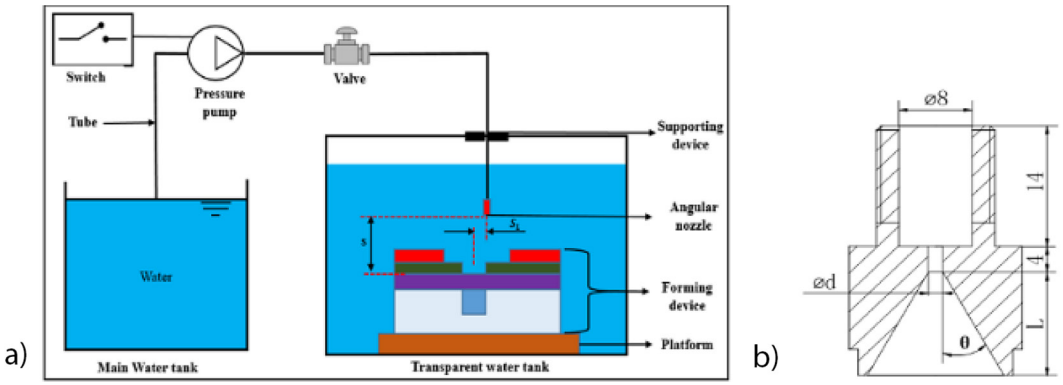

Figure 3. (a) Experimental system of water jets cavitation shock micro-forming; and (b) Nozzle geometry diagram

which can analyze the mechanical properties of the material. The entire test process includes loading and unloading processes. Through the analysis of the material loading and unloading curves, its mechanical properties, including nano-hardness and elastic modulus, could be obtained. The nano-hardness H and elastic modulus E_r of the material in the experiment could be obtained by the following formula [19]:

$$H = \frac{P_{max}}{A} = \frac{P_{max}}{\pi\alpha^2}$$
$$E_r = \frac{1-v_1^2}{E_1} + \frac{1-v_2^2}{E_2} \quad (1)$$
$$S = \frac{dP}{dh} = \frac{2}{\sqrt{\pi}} E_r \sqrt{A}$$

where: $Pmax$ – the maximum pressure,
E_1 and v_1 – the elastic modulus and Poisson's ratio of the material,
A – the contact area projected by the indenter, E_2
v_2 – the elastic modulus and Poisson's ratio of the indenter. For the diamond indenter,
E_2 = 1140GPa,
v_2 = 0.07.
The elastic contact stiffness is the slope at the start of the unloading slope,
E_r – the indenter system's efficient Young's modulus, and the contact radius α and contact depth relationship is:

$$\alpha = h_c tan\theta \quad (2)$$

where: in the formula, for the ideal Brinell pin half-taper angle θ = 70.30°.

According to the 'Oliver-Pharr' [20] method, the indentation depth of the material should be kept below 5% of the original material thickness, which can ignore the influence of the elastic deformation of the material on the test results [21]. This section uses a nano-indentation instrument to test the cross-section of the AISI 304 stainless steel foil micro-formed parts and then obtains the nano-hardness value of the AISI 304 stainless steel foil after cavitation water jet shock.

Nano-hardness test

In this section, for the AISI 304 stainless steel foil micro-formed parts, the fillet area, transition area, and bottom area of the formed part were selected as the location of the nano-indentation test point, as shown in Figure 4. Taking into account the accuracy of the measurement results, continue to measure around the test location (upper and lower every 10 μm), of the fillet, transitional and bottom regions and finally the average value of the final test result was taken. The formed parts with incident pressures of 8 MPa and 20 MPa were measured respectively. Figure 4(b) shows the actual location of the nano-indentation test point in the bottom area of the formed part after impact under an incident pressure of 20 MPa.

RESULTS AND DISCUSSION

Analysis of nano-indentation experiment results

The load-displacement curve obtained after the nano-indentation test is shown in Figure 5. Figure 5(a) shows the loading and unloading curves of the AISI 304 stainless steel foil substrate. It can

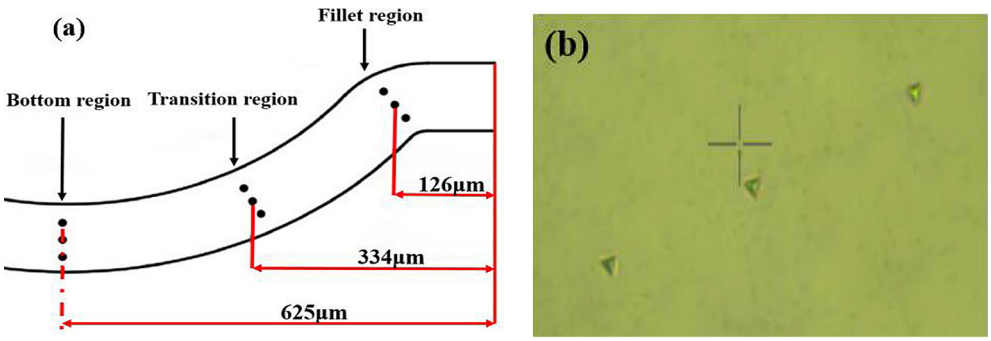

Figure 4. Schematic diagram of a nano-indentation test, (a) the location of the nano-indentation test point, (b) the actual location of the test point at the bottom region

be seen that the hardness of the AISI 304 stainless steel foil substrate was small and the contact depth was relatively large. Three curves A, B and C in Figure 5b are the nano-indentation loading and unloading curves of AISI 304 stainless steel foil under unshocked region, 8MPa, and 20MPa incident pressure. The maximum indentation depth of formed samples after water jet shock reduced from the fillet region to the bottom region, with their corresponding values decreasing from

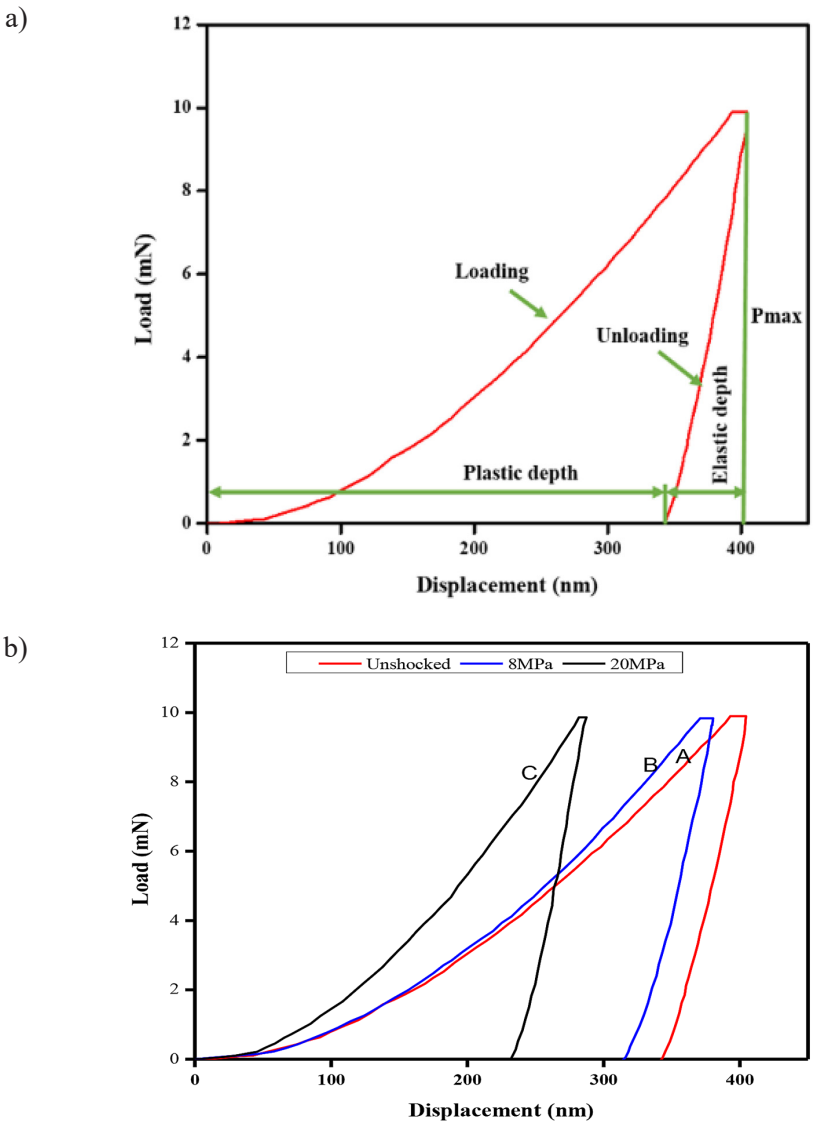

Figure 5. (a) The nano-indentation curve of the raw materials, (b) the nano-indentation curve with different incident pressure conditions

Table 1. Nano-hardness and modulus of elasticity in the forming area

Incident pressure (MPa)	Nano-hardness, H(MPa)			Elastic modulus, Er(GPa)		
	Bottom region	Transition region	Fillet region	Bottom region	Transition region	Fillet region
~	2745.7			87.7		
8	3130.7	3214.8	3589.8	92.4	94.9	98.1
20	6048.7	6108.6	6435.9	153.1	162.6	166.2

3589.8 MPa to 3130.7 MPa at the incident pressure of 8 MPa, as compared to the measurement findings of the unformed sections. It can be seen from the curve in Figure 5b that the loading and unloading curves are continuous and there is no springback phenomenon, indicating that the material has good elastic properties. The numerical values of the nano-hardness and elastic modulus of the forming area are listed in Table 1.

Figure 6 shows the distribution of nano-hardness and elastic modulus of the cross-section of AISI 304 stainless steel foil micro-formed parts [22]. The experimental results show that the nano-hardness and elastic modulus of AISI 304 stainless steel foil micro-formed parts were greatly improved as compared with those before impact forming. Before impact, the nano-hardness and elastic modulus of AISI 304 stainless steel foil was 2745.7 MPa and 87.7 GPa respectively. Under the incident pressure of 8 MPa, the nano-hardness values of the bottom area, transition area and fillet area of the formed parts were 3130.7 MPa, 3214.8 MPa, and 3589.8 MPa respectively increased by 13.8%, 16.6%, and 30.5% before the same cavitation water jet shock. The elastic modulus was 92.4 GPa, 94.9 GPa, and 98.1 GPa respectively, increased by 5.3% before the same cavitation water jet shock of 8.3% and 12.4%. The experimental data clearly shows that the hardness and elastic modulus of the unshocked area are both less than the sample after impact under the incident pressure of 8 MPa, 12 MPa, 16 MPa and 20 MPa. Moreover, the hardness of the cross-section increases with the increase of the incident pressure from 8 MPa, 12 MPa, and 16 MPa to 20 MPa at high incident pressure. The hardness of the cross-section also increased. Therefore, the increase of nano-hardness can not only enhance the surface strength of the material but also prevent the material from separating from the surface. In summary, the surface hardness of AISI 304 stainless steel foil greatly improved in the process of cavitating water jet micro-forming, and the effect of forming and strengthening was achieved [23, 24]. In addition, the elastic modulus during the forming process significantly improved, and the comprehensive mechanical properties of the parts formed by the cavitation water jet shock micro-forming improved.

SEM analysis

To conduct an in-depth study on the deformation of the workpiece, this part of the study uses scanning electron microscopy (SEM) to observe the microscopic morphology of the

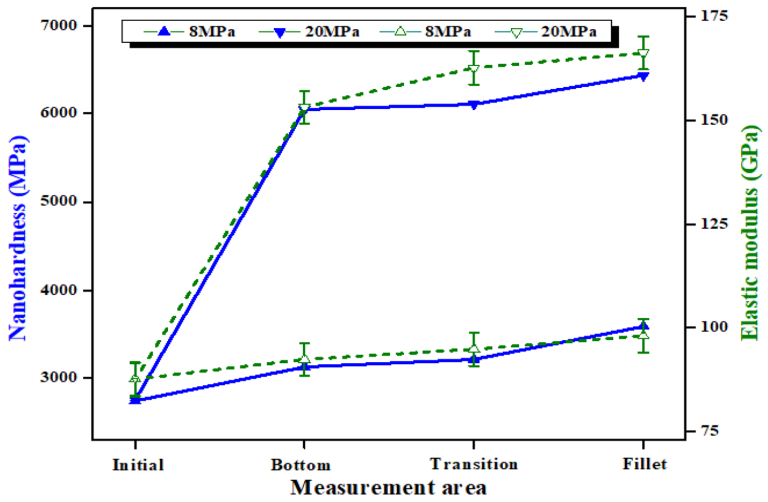

Figure 6. The distribution of nano-hardness and elastic modulus of micro section

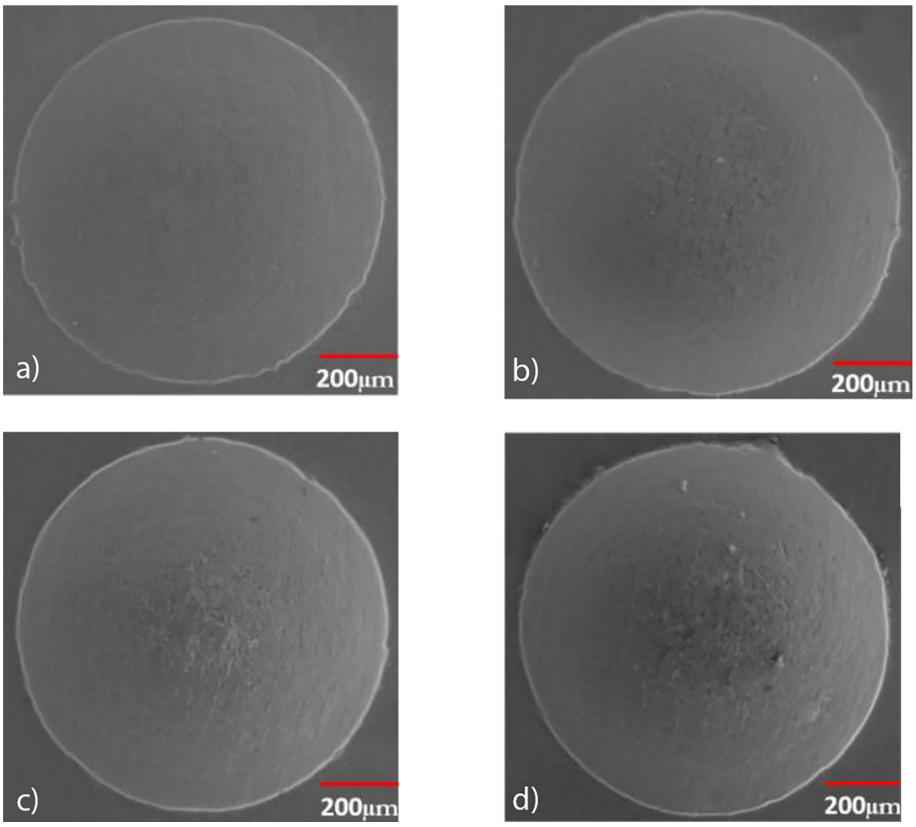

Figure 7. The bottom morphology of the micro-formed parts, (a) 8 MPa, 88.5 μm, (b) 12 MPa, 145.0 μm, (c) 16 MPa, 169.4 μm, (d) 20 MPa, 226.1 μm

workpiece surface under different incident pressures. Figure 7 shows the morphology of AISI 304 stainless steel foil micro-formed parts under different incident pressures. The experimental results showed that with the increase of the incident pressure of 8 MPa, 12 MPa, 16 MPa and 20MPa their corresponding forming depth value increased from 88.5 μm, 145.0 μm, 169.4 μm, and 226.1 μm as shown in Figure 7. This indicates that the surface morphology of AISI 304 stainless steel foil micro-formed parts changed from spherical to spherical, and the bottom of the micro-formed parts had defects with varying degrees as the incident pressures increased.

Figure 8 shows that the defects at the bottom of AISI 304 stainless steel foil micro-formed parts were significantly expanded, which may cause micro-layer cracking with the increase of incident pressure. When the high-pressure shock wave generated by the collapse of the bubble acts on the target surface, a reflected shock wave will appear. When the reflected shock wave and the subsequent shock wave collide on the target surface, the two will superimpose each other, thereby forming high tensile stress. If the tensile stress exceeds the peak tensile strength of the target material and acts on the surface of the material multiple times, micro-cracks will eventually appear. If a large or deep crack occurs, it will detach from the surface of the material, and eventually, a microlayer crack will appear. The crack structure may be due to the target material undergoing plastic deformation under the action of high-pressure shockwaves, and its surface is convex. However, the tensile stress at the bottom of the outer surface of the target and the compressive stress on the inner surface lead to some small defects on the bottom surface and then some resembling crack structures were formed.

CONCLUSIONS

This paper demonstrates the effects of the incident pressure on the micro-forming properties of metallic foils with cavitating water jet shock. Studies were on the nano-hardness, elastic modulus, and SEM analysis of the formed parts. The following conclusions were drawn. During the micro-forming process of cavitation water jet shock on metallic foils, the nano-hardness and elastic modulus increased significantly with an

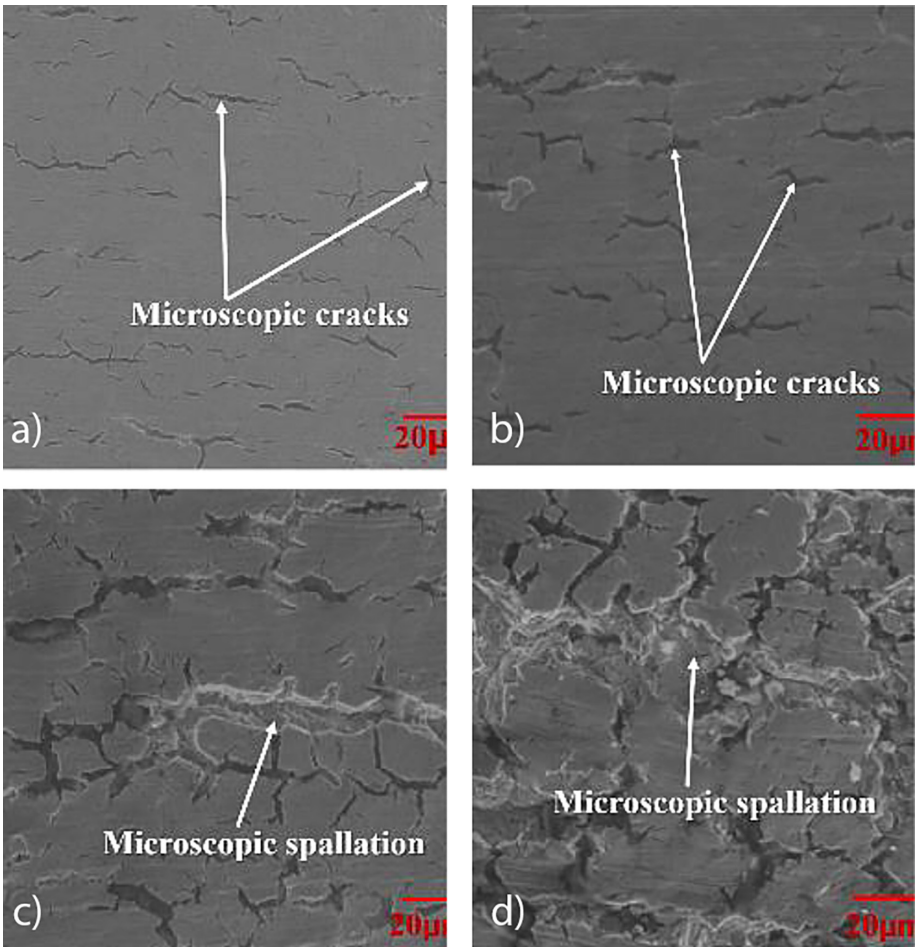

Figure 8. Defects at the bottom of micro formed parts, (a) 8 MPa, 88.5 μm, (b) 12 MPa, 145.0 μm, (c) 16 MPa, 169.4 μm, (d) 20 MPa, 226.1 μm

increase in the incident pressure. When the incident pressure was 20 MPa and the impact time of 5 min, the hardness increased by at least 122%, and the elastic modulus increased by at least 76%. After the cavitation water jet shocked the metallic foil of the SEM analysis and the results indicated that, as the incident pressure increases, the surface morphology of the formed part changes from approximately spherical to spherical, and the spherical roundness increases. In addition, there are different degrees of defects at the bottom of the formed part, and as the incident pressure increases, the bottom defects became more and more obvious, from micro-cracks to micro-layer cracks.

REFERENCES

1. Szala M., Walczak M., Hejwowski T. Factors influencing cavitation erosion of NiCrSiB hardfacings deposited by oxy-acetylene powder welding on grey cast iron. Advances in Science and Technology. Research Journal, 2021; 15.
2. Soyama H., Park J., Saka M. Use of cavitating jet for introducing compressive residual stress. Journal of manufacturing science and engineering, 2000; 122: 83–89.
3. Adem Musliu A.M., Bekim M., Naim B. Analysis of Research of Heavy Metals On Ground In "Kosova-A" Thermal Power Plant. International Journal of Applied Physics, 2022; 7: 24–35.
4. Huang Y.C., Hammitt F., Yang W. Hydrodynamic phenomena during high-speed collision between liquid droplet and rigid plane, 1973.
5. Tong R., Schiffers W.P., Shaw S.J., Blake J.R., Emmony D. The role of 'splashing'in the collapse of a laser-generated cavity near a rigid boundary. Journal of Fluid Mechanics, 1999; 380: 339–361.
6. Wang P., Shi D., Cui X., Su B., Li G., He D. Study on the physical mechanism of water layer on the morphological evolution of transient-pulse high-speed water jet. Ocean Engineering, 2023; 267: 113238.
7. Quaisie J.K., Yun W., Zhenying X., Chao Y., Li F., Baidoo P., et al. Experimental Study on Water-Jet

Shock Microforming Process Using Different Incident Pressures. Advances in Materials Science and Engineering, 2020.

8. Matuszak J. Effect of Ceramic Brush Treatment on the Surface Quality and Edge Condition of Aluminium Alloy after Abrasive Waterjet Machining. Advances in Science and Technology Research Journal, 2021; 15.
9. Cheng F., Ji W., Qian C., Xu J. Cavitation bubbles dynamics and cavitation erosion in water jet. Results in Physics, 2018; 9: 1585–1593.
10. Hao C., Cheng Y., Wang L., Liu H., Shang Z. A novel technology for enhancing coalbed methane extraction: Hydraulic cavitating assisted fracturing. Journal of Natural Gas Science and Engineering, 2019; 72: 103040.
11. Xiang M., Cui J., Yang Y., Liao Y., Wang K., Chen Y., et al. Shock responses of nanoporous aluminum by molecular dynamics simulations. International Journal of Plasticity, 2017; 97: 24–45.
12. Errandonea D., Garg A.B. Recent progress on the characterization of the high-pressure behaviour of AVO4 orthovanadates. Progress in Materials Science, 2018; 97: 123–169.
13. Brujan E.-A. Shock wave emission and cavitation bubble dynamics by femtosecond optical breakdown in polymer solutions. Ultrasonics Sonochemistry, 2019; 58: 104694.
14. Fuentes G.G. Chapter 20 – Surface Engineering and Micro-manufacturing," in Micromanufacturing Engineering and Technology (Second Edition), Y. Qin, Ed., ed Boston: William Andrew Publishing, 2015; 459–486.
15. Sato K., Sugimoto Y., Ohjimi S. Pressure-wave formation and collapses of cavitation clouds impinging on solid wall in a submerged water jet, 2009.
16. Soyama H. Effect of nozzle geometry on a standard cavitation erosion test using a cavitating jet. Wear, 2013; 297: 895–902.
17. Sharifikolouei E., Sarac B., Micoulet A., Mager R., Watari-Alvarez M., Hadjixenophontos E., et al. Improvement of hardness in Ti-stabilized austenitic stainless steel. Materials & Design, 2022; 223: 111242.
18. Sonmez F.O., Demir A. Analytical relations between hardness and strain for cold formed parts," Journal of materials processing technology, 2007; 186: 163–173.
19. Szala M., Walczak M., Pasierbiewicz K., Kamiński M. Cavitation erosion and sliding wear mechanisms of AlTiN and TiAlN films deposited on stainless steel substrate. Coatings, 2019; 9: 340.
20. Oliver W.C., Pharr G.M. An improved technique for determining hardness and elastic modulus using load and displacement sensing indentation experiments. Journal of materials research, 1992; 7: 1564–1583.
21. Cheng Y.-T., Cheng C.-M. Scaling, dimensional analysis, and indentation measurements. Materials Science and Engineering: R: Reports, 2004; 44: 91–149.
22. Liu H., Sun X., Shen Z., Li L., Sha C., Ma Y., et al. Experimental and Numerical Simulation Investigation on Laser Flexible Shock Micro-Bulging, 2017; 7.
23. Tromas C., Stinville J.C., Templier C., Villechaise P. Hardness and elastic modulus gradients in plasma-nitrided 316L polycrystalline stainless steel investigated by nanoindentation tomography. Acta Materialia, 2012; 60: 1965–1973.
24. Czapczyk K., Siwak P., Legutko S. Study of the effect of the electroless ni-p coating thickness applied on aw-7075 aluminium alloy on its mechanical properties. Advances in Science and Technology. Research Journal, 2018; 12: 291–297